THE JOURNAL OF BIOLOGICAL CHEMISTRY VOL. 290, NO. 25, pp. 15475–15486, June 19, 2015

UDP-galactose (SLC35A2) and UDP-*N*-acetylglucosamine (SLC35A3) Transporters Form Glycosylation-related Complexes with Mannoside Acetylglucosaminyltransferases (Mgats)*

Received for publication, January 5, 2015, and in revised form, April 28, 2015 Published, JBC Papers in Press, May 5, 2015, DOI 10.1074/jbc.M115.636670

Dorota Maszczak-Seneczko[‡1], Paulina Sosicka[‡1], Beata Kaczmarek[‡], Michał Majkowski[§], Marcin Luzarowski[‡], Teresa Olczak[‡], and Mariusz Olczak[‡2]

From the Laboratories of [‡]Biochemistry and [§]Cytobiochemistry, Faculty of Biotechnology, University of Wroclaw, 50-383 Wroclaw, Poland

Background: UDP-galactose (UGT) and UDP-*N*-acetylglucosamine (NGT) transporters and mannoside acetylglucosaminyltransferases (Mgats) are important mediators of *N*-linked protein glycosylation.
Results: UGT and NGT are in close proximity to Mgats.
Conclusion: UGT, NGT and Mgats may form multiprotein complexes mediating biosynthesis of *N*-glycans.
Significance: Protein-protein interactions between Golgi-resident nucleotide sugar transporters and glycosyltransferases appears to be an inherent feature of *N*-linked glycosylation.

UDP-galactose transporter (UGT; SLC35A2) and UDP-*N*-acetylglucosamine transporter (NGT; SLC35A3) form heterologous complexes in the Golgi membrane. NGT occurs in close proximity to mannosyl (α-1,6-)-glycoprotein β-1,6-*N*-acetylglucosaminyltransferase (Mgat5). In this study we analyzed whether NGT and both splice variants of UGT (UGT1 and UGT2) are able to interact with four different mannoside acetylglucosaminyltransferases (Mgat1, Mgat2, Mgat4B, and Mgat5). Using an *in situ* proximity ligation assay, we found that all examined glycosyltransferases are in the vicinity of these UDP-sugar transporters both at the endogenous level and upon overexpression. This observation was confirmed via the FLIM-FRET approach for both NGT and UGT1 complexes with Mgats. This study reports for the first time close proximity between endogenous nucleotide sugar transporters and glycosyltransferases. We also observed that among all analyzed Mgats, only Mgat4B occurs in close proximity to UGT2, whereas the other three Mgats are more distant from UGT2, and it was only possible to visualize their vicinity using proximity ligation assay. This strongly suggests that the distance between these protein pairs is longer than 10 nm but at the same time shorter than 40 nm. This study adds to the understanding of glycosylation, one of the most important post-translational modifications, which affects the majority of macromolecules. Our research shows that complex formation between nucleotide sugar transporters and glycosyltransferases might be a more common phenomenon than previously thought.

Glycosylation of macromolecules plays an essential role in the growth and development of eukaryotes, as well as in host-pathogen interactions. This protein post-translational modification increases solubility and structural stability, protects against proteolysis, and assists in protein folding. It also plays a crucial role in the immune response, cell-cell and cell-extracellular matrix recognition, and selective protein targeting (1). The glycan moiety is synthesized and modified by glycosyltransferases acting in the lumen of the endoplasmic reticulum (ER)[3] and Golgi apparatus. Substrates required in the glycosylation process are sugars activated by the addition of CMP, GDP, or UDP. Nucleotide sugars are synthesized in the cytosol (2), except for CMP-sialic acid, which is the only nucleotide sugar synthesized in the nucleus (3). To be delivered into the ER and Golgi lumen, where glycosylation occurs, they need to be transferred across membranes of these organelles. Nucleotide sugar transporters (NSTs) play an essential role in this process (4, 5). It has been proposed that they act as antiporters, exchanging nucleotide sugar with the corresponding nucleoside monophosphate, which is a product of the glycosylation reaction (6).

NSTs are hydrophobic proteins with molecular masses of 30–45 kDa. It is predicted that they belong to type III multitransmembrane proteins, with an even number of transmembrane domains and both N and C termini facing the cytosol. The topology of murine CMP-sialic acid transporter has been experimentally determined. This protein has 10 transmem-

* This work was supported by Grant 2011/03/B/NZ1/02084 from the National Science Center (Krakow, Poland). Publication costs were supported by Wroclaw Center of Biotechnology program of the Leading National Research Center (KNOW) for 2014–2018.
[1] These authors contributed equally to this study and share the first authorship.
[2] To whom correspondence should be addressed: Lab. of Biochemistry, Faculty of Biotechnology, University of Wroclaw, 14A F. Joliot-Curie St., 50-383 Wroclaw, Poland. Tel.: 48-713752-710; Fax: 48-713752-608; E-mail: Mariusz.Olczak@biotech.uni.wroc.pl.

[3] The abbreviations used are: ER, endoplasmic reticulum; NST, nucleotide sugar transporter; UGT, UDP-galactose transporter (SLC35A2); NGT, UDP-*N*-acetylglucosamine transporter (SLC35A3); FLIM, fluorescence lifetime imaging microscopy; FRET, fluorescence resonance energy transfer; eGFP, enhanced green fluorescent protein; mRFP, monomeric red fluorescent protein; PLA, *in situ* proximity ligation assay; Mgat, mannoside acetylglucosaminyltransferase; Mgat1, mannosyl (α-1,3-)-glycoprotein β-1,2-*N*-acetylglucosaminyltransferase; Mgat2, mannosyl (α-1,6-)-glycoprotein β-1,2-*N*-acetylglucosaminyltransferase; Mgat4, mannosyl (α-1,3-)-glycoprotein β-1,4-*N*-acetylglucosaminyltransferase; Mgat5, mannosyl (α-1,6-)-glycoprotein β-1,6-*N*-acetylglucosaminyltransferase.

TABLE 1
List of expression plasmids used in this study

Plasmid name	Original vector	Insert	Reference
pSelect-RFP-NGT	pSelect	RFP-NGT	Ref. 15
pTag-RFP-C-UGT1	pTag-RFP-C	UGT1	Ref. 13
pTag-RFP-C-UGT2	pTag-RFP-C	UGT2	Ref. 13
pTag-GFP2-C-Mgat1	pTag-GFP2-C	Mgat1	This study
pTag-GFP2-C-Mgat2	pTag-GFP2-C	Mgat2	This study
pTag-GFP2-C-Mgat4B	pTag-GFP2-C	Mgat4B	This study
pTag-GFP2-C-Mgat5	pTag-GFP2-C	Mgat5	Ref. 15
pSelect-HA-NGT	pSelect	HA-NGT	This study
pSelect-HA-UGT1	pSelect	HA-UGT1	This study
pSelect-HA-UGT2	pSelect	HA-UGT2	This study
3×FLAG-CMV-26-Mgat1	3 × FLAG-myc-CMV-26[a]	Mgat1	This study
3×FLAG-CMV-26-Mgat2	3 × FLAG-myc-CMV-26[a]	Mgat2	This study
3×FLAG-CMV-26-Mgat4B	3 × FLAG-myc-CMV-26[a]	Mgat4B	This study
3×FLAG-CMV-26-Mgat5	3 × FLAG-myc-CMV-26[a]	Mgat5	This study
3×FLAG-CMV-26-SLC35B4	3 × FLAG-myc-CMV-26[a]	SLC35B4	Ref. 24
3×FLAG-CMV-26-UGT2	3 × FLAG-myc-CMV-26[a]	UGT2	Ref. 24

[a] Only 5′ sequence encoding N-terminal 3×FLAG was attached to the insert.

brane domains and both N and C termini on the cytosolic side of the Golgi membrane (7). Several studies have demonstrated that NSTs function in the form of homodimers (8–10) or higher homooligomers (11, 12). Recently, it has been discovered that NSTs are also able to form heterologous complexes (13). Moreover, there are two reports on the interactions between NSTs and respective glycosyltransferases (14, 15). However, in both cases, the results were derived from overexpression experiments.

One of the best characterized NSTs is mammalian UDP-galactose transporter (UGT; SLC35A2). In human tissues, the CHO and MDCK cell lines, two splice variants (UGT1 and UGT2) of this transporter have been identified (16–19). Detailed study on UDP-galactose transporter was possible because of the generation of mammalian cell lines deficient in UGT, such as MDCK cells resistant to *Ricinus communis* agglutinin (MDCK-RCA^r) (20), CHO-Lec8 (21), and Had-1 (22, 23) cells. In contrast, little is known about mammalian UDP-*N*-acetylglucosamine transporter (NGT; SLC35A3). This protein has been shown to be localized to the Golgi apparatus of MDCK-RCA^r cells (24) and to partially correct the galactosylation defect when overexpressed in UGT-deficient mammalian cell lines (25). Our recent studies demonstrated that NGT and UGT are able to form heterologous complexes in the Golgi membrane, and their role in glycosylation is coupled (13, 26, 27).

Glycosyltransferases are essential in glycan moiety synthesis. Most of them are N_{in}/C_{out} (type II) membrane proteins with a short N-terminal cytoplasmic domain, a single membrane-spanning domain, and a large catalytic domain in the Golgi or ER lumen (28–30). The catalytic domain is linked to the transmembrane domain by the so-called "stem" region. This region is thought to mediate positioning of the catalytic part of glycosyltransferases away from the lipid bilayer, facilitating access to the substrate (31).

Mannoside acetylglucosaminyltransferases (Mgats) are Golgi-resident glycosyltransferases that participate in the first stage of complex *N*-glycan biosynthesis. Mono- and diantennary glycans are formed by the action of mannosyl (α-1,3-)-glycoprotein β-1,2-*N*-acetylglucosaminyltransferase (Mgat1) and mannosyl (α-1,6-)-glycoprotein β-1,2-*N*-acetylglucosaminyltransferase (Mgat2), whereas further branching is performed by mannosyl (α-1,3-)-glycoprotein β-1,4-*N*-acetylglucosaminyltransferase (Mgat4) and mannosyl (α-1,6-)-glycoprotein β-1,6-*N*-acetylglucosaminyltransferase (Mgat5), resulting in respective formation of tri- and tetraantennary structures. It is worth noting that Mgat1 and Mgat2 have been reported to display lower K_m values for UDP-*N*-acetylglucosamine than Mgat4 and Mgat5, both of which are believed to be limited by concentrations of this nucleotide sugar (32).

Our recent findings strongly suggest that NGT occurs in close proximity to Mgat5 (15) and NGT and UGT form heterologous complexes in the Golgi membrane (13). Based on our previous observations, we aimed to investigate whether these NSTs interact with mannoside acetylglucosaminyltransferases mediating *N*-glycan biosynthesis, *i.e.* Mgat1, Mgat2, Mgat4B, and Mgat5.

Experimental Procedures

Construction of Expression Plasmids—Plasmids designed and constructed or used in this study are listed in Table 1. Detailed information regarding sequences of primers, sequences of prepared constructs, and the cloning strategy is available upon request.

Cell Maintenance and Transfection—For the *in situ* proximity ligation assay (PLA) with antibodies against endogenous proteins, PC-3 cells were grown in DMEM supplemented with 10% fetal bovine serum, 4 mM L-glutamine, 100 units/ml penicillin, and 100 μg/ml streptomycin. For PLA experiments employing overexpressed proteins, MDCK-RCA^r cells were grown and stably transfected with plasmids enabling expression of FLAG-tagged Mgats as described previously (24). Stable transfectants expressing either Mgat1, Mgat2, Mgat4B, or Mgat5 were selected in complete medium containing 600 μg/ml G-418 sulfate (InvivoGen). Afterward, cells expressing one of the listed Mgats were transiently transfected with pSelect plasmid encoding a sequence of either NGT, UGT1, or UGT2. PLA analyses were conducted 48 h after transfection.

As positive and negative PLA controls, MDCK-RCA^r cells stably transfected with plasmids enabling expression of either FLAG-tagged UGT2 (positive control) or FLAG-tagged SLC35B4 (negative control) were employed (24). Cells expressing FLAG-SLC35B4 were co-transfected with pSelect expression plasmids as described above.

TABLE 2
List of antibodies used in *in situ* PLA experiments

Antibody	Monoclonal	Dilution	Host	Source
Anti-FLAG	Yes	1:100	Mouse	Sigma-Aldrich
Anti-HA	No	1:500	Rabbit	Abcam
Anti-Mgat1	No	1:50	Mouse	Abcam
Anti-Mgat2	Yes	1:50	Mouse	Abnova
Anti-Mgat4B	No	1:50	Mouse	Abnova
Anti-Mgat5	Yes	1:20	Mouse	R&D Systems
Anti-SLC35A2	No	1:50	Rabbit	Abcam
Anti-SLC35A3	No	1:50	Rabbit	Abcam

For FLIM-FRET experiments, HEK293T cells were grown in DMEM supplemented with 10% fetal bovine serum, 4 mM L-glutamine, 100 units/ml penicillin, and 100 μg/ml streptomycin and transiently transfected with expression plasmid(s) as described previously (15). FLIM-FRET analysis was performed 48 h after transfection.

In Situ Proximity Ligation Assay—PLA experiments were performed using Duolink reagents according to the original protocol (Sigma-Aldrich). Briefly, MDCK-RCA^r cells stably transfected with plasmids enabling expression of one of the analyzed Mgats or SLC35B4 in fusion with the FLAG epitope were grown on 8-well microscope slides (Merck Millipore) for 2 days after transient transfection with the pSelect plasmid encoding the UDP-sugar transporter (either NGT, UGT1, or UGT2) in fusion with HA peptide. Alternatively, for PLA analysis using antibodies targeting endogenous proteins, PC-3 cells were seeded on 8-well microscope slides and grown for 2 days. Afterward, cells were fixed with 4% (v/v) paraformaldehyde solution in PBS for 20 min at room temperature and permeabilized for 5 min using 0.1% (v/v) Triton X-100 in PBS at room temperature. Nonspecific binding sites were blocked with 10% (v/v) normal goat serum in PBS for 1 h at room temperature. After blocking, slides were incubated for 2 h with an appropriate pair of mouse and rabbit primary antibodies (Table 2) at 37 °C. Then cells were incubated with anti-mouse PLA probe MINUS and anti-rabbit PLA probe PLUS (both diluted 1:5 in 10% (v/v) normal goat serum) for 1 h at 37 °C. Between all these steps, slides were washed with PBS three times for 5 min. After incubation with PLA probes, cells were washed twice with 1× concentrated buffer A for 5 min and incubated with ligation solution for 30 min at 37 °C. Subsequently, slides were washed twice with 1× concentrated buffer A for 2 min and incubated with amplification solution (detection reagent Orange containing fluorophore characterized by excitation maximum of 554 nm and emission maximum of 576 nm was employed) for 100 min at 37 °C. Ultimately, cells were washed twice with 1× concentrated buffer B for 10 min and once with 0.01× concentrated buffer B for 1 min, mounted onto glass coverslips using Duolink *in situ* mounting medium with DAPI, and examined with a ZEISS LSM 510 confocal microscope.

Alternatively, as a PLA-positive control, we used cells overexpressing UGT2 with the N-terminally fused FLAG epitope. After blocking, cells were incubated with epitope-specific mouse monoclonal antibody and rabbit polyclonal antibodies raised against the C-terminal part of SLC35A2 (Table 2). The rest of the experimental procedure remained unchanged.

Confocal and Fluorescence Lifetime Imaging Microscopy—Confocal and FLIM microscopy were performed as described previously (13, 15), except that HEK293T cells were used in all experiments, and cells transiently transfected with expression plasmids listed in Table 1 were seeded onto 35-mm CELLview glass bottom dishes (Greiner Bio-One) prior to imaging. Analysis of the data received from FLIM-FRET experiments was carried out as reported previously (13), except that a bi-exponential model was employed during data interpretation for eGFP-Mgat/mRFP-NST combinations with fixed donor lifetime values derived from control measurements (eGFP-Mgat only) as τ_{long}. Mean FRET efficiency was calculated from the following equation: $1 - (\tau_{short}/\tau_{long})$, where τ_{short} symbolizes fluorescence lifetime of the interacting donor fraction (f_{short}), and τ_{long} indicates the fluorescence lifetime of the noninteracting donor fraction.

Statistical Analysis—To analyze whether the differences in mean eGFP fluorescence lifetimes (τ) between control measurements (eGFP-Mgat only) and investigated samples, where the acceptor was present (eGFP-Mgat+mRFP-NST), are statistically significant, one-way analysis of variance was employed. All statistical analyses were performed using GraphPad Prism software (GraphPad Prism Inc.).

Results and Discussion

The formation of homo- and heterooligomeric complexes is a common phenomenon among mammalian (33–35) and plant (36, 37) glycosyltransferases, which is believed to prevent entry into the secretory pathway, thus supporting maintenance of a definite location within the Golgi apparatus. It has been demonstrated that also NSTs have a tendency to homooligomerize. The first findings, in the late 1990s, demonstrated dimer formation by UDP-*N*-acetylgalactosamine transporter (10), as well as GDP-fucose transporter (9) isolated from rat liver. GDP-mannose transporter from *Saccharomyces cerevisiae* exhibits a similar tendency (8). Interestingly, a homologous protein from *Leishmania donovani* forms hexamers (11). Oligomeric structures have also been described for canine UGT (12) and human NGT (13). It has been proposed that oligomerization of NSTs allows for the formation of transmembrane channels enabling import of nucleotide sugars (38).

Recently, we found that NGT forms heterologous complexes with UGT1 and UGT2 (13). This is the first described phenomenon of an interaction between two distinct NSTs. It has also been reported that some NSTs are able to interact with functionally related glycosyltransferases. The first finding describes an association between UDP-galactose:ceramide galactosyltransferase and UGT (14). The second report, coming from our laboratory, showed that NGT is in close proximity to Mgat5 (15). However, both findings refer to the experiments performed only on overexpressed proteins.

All observations mentioned above encouraged us to investigate whether other mannoside acetylglucosaminyltransferases (Mgat1, Mgat2, and Mgat4) also occur in close proximity to NGT. Based on our recent discovery of NGT/UGT heterologous complexes, we also tested whether examined Mgats are in close proximity to both UGT splice variants. Among Mgat4 isoforms, Mgat4A expression appears to be tissue-specific,

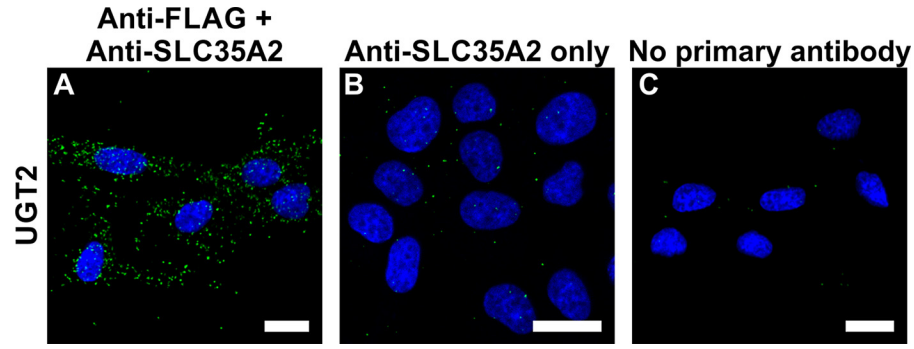

FIGURE 1. ***In situ* PLA controls.** *A*, PLA analysis of UGT2 N and C terminus proximity performed in MDCK-RCA^r cells. *B*, negative control where anti-FLAG antibody was omitted during the PLA procedure. *C*, negative control where both primary antibodies were omitted during the PLA procedure. *Bars*, 20 μm.

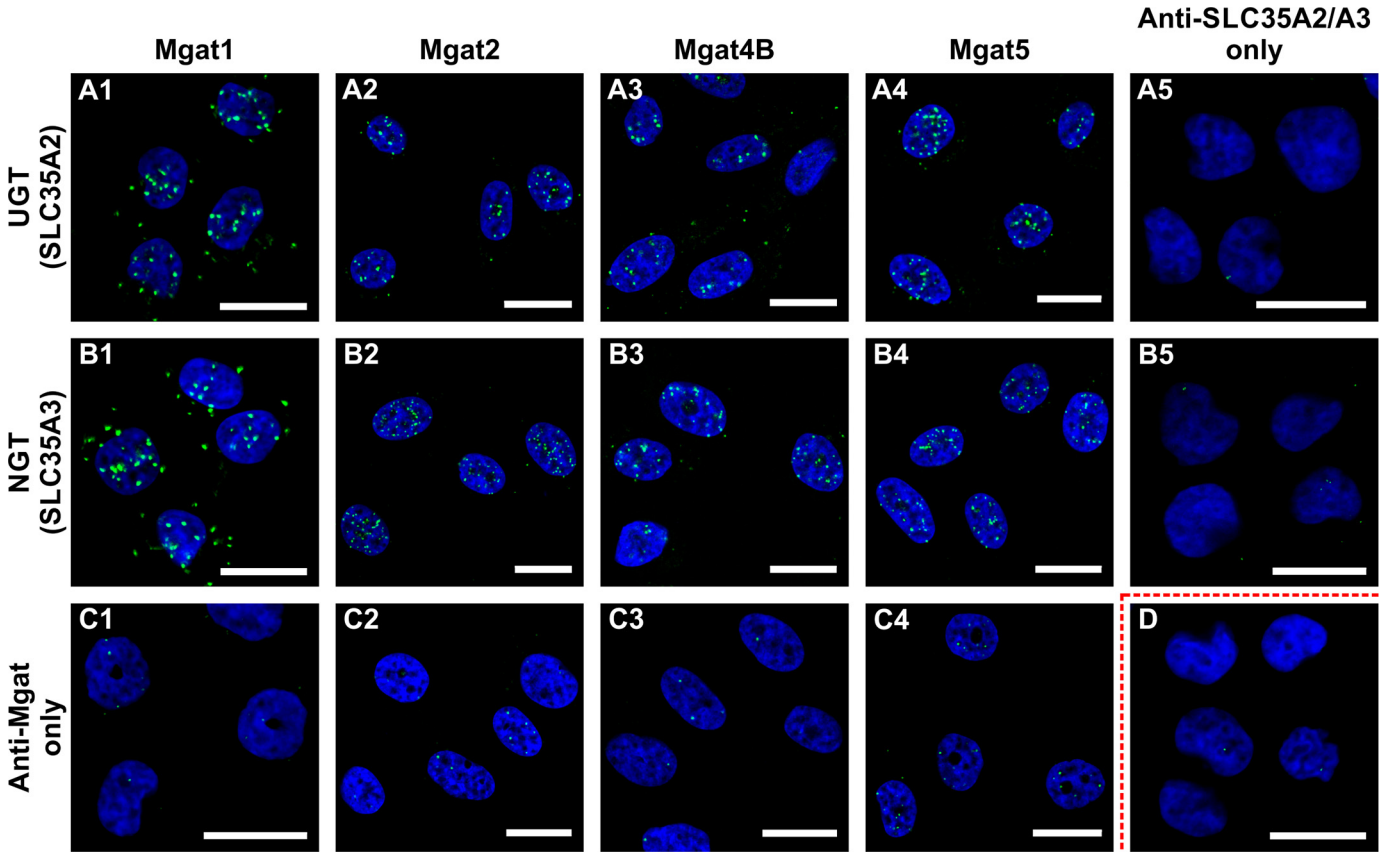

FIGURE 2. **Visualization of interactions between endogenous Mgats and UDP-sugar transporters using *in situ* PLA.** *A* and *B*, PLA analysis of either Mgat1 (*panels 1*), Mgat2 (*panels 2*), Mgat4B (*panels 3*), or Mgat5 (*panels 4*) interaction with UGT (*A*) and NGT (*B*) in PC-3 cell line. *C*, negative control for Mgats-UDP-sugar transporters interaction analysis, where primary antibody against Mgat1/Mgat2/Mgat4B/Mgat5 was not added during the PLA procedure. Negative control for Mgat-UDP-sugar transporters interaction analysis, where primary antibody against UGT/NGT was not added during the PLA procedure (*panels 5*). *D*, negative control for Mgat-UDP-sugar transporters interaction where both primary antibodies were omitted during the PLA procedure. *Bars*, 20 μm.

whereas Mgat4B is more ubiquitously expressed (39, 40). Our previous attempts to overexpress eGFP-tagged Mgat4A in different cell lines resulted in apparent mislocalization of the fusion protein (data not shown); therefore in this study we acknowledged Mgat4B as a more representative Mgat4 isoform.

The In Situ PLA Reveals Close Proximity between UDP-Sugar Transporters and Mgats—PLA allows one to visualize close (up to 40 nm) proximity between two proteins in fixed cells. When two proteins are in proximity, PLA probe PLUS and PLA probe MINUS are close enough to form a circular DNA structure, which can be amplified after ligation using polymerase solution. In amplification solution, a fluorophore-tagged DNA probe is also present, whose sequence is complementary to the one being amplified; that is why the probe can bind to it, which allows one to visualize the close proximity between two investigated proteins.

First, we performed a positive control using MDCK-RCA^r cells stably expressing UGT2 in N-terminal fusion with the FLAG epitope to verify whether PLA is a suitable method in our study and develop experimental procedure conditions. We used antibodies raised against the UGT C terminus together with anti-FLAG antibodies. Previously, we were able to detect close proximity between fluorescent proteins attached to the N and C termini of UGT (our unpublished data). As expected, a

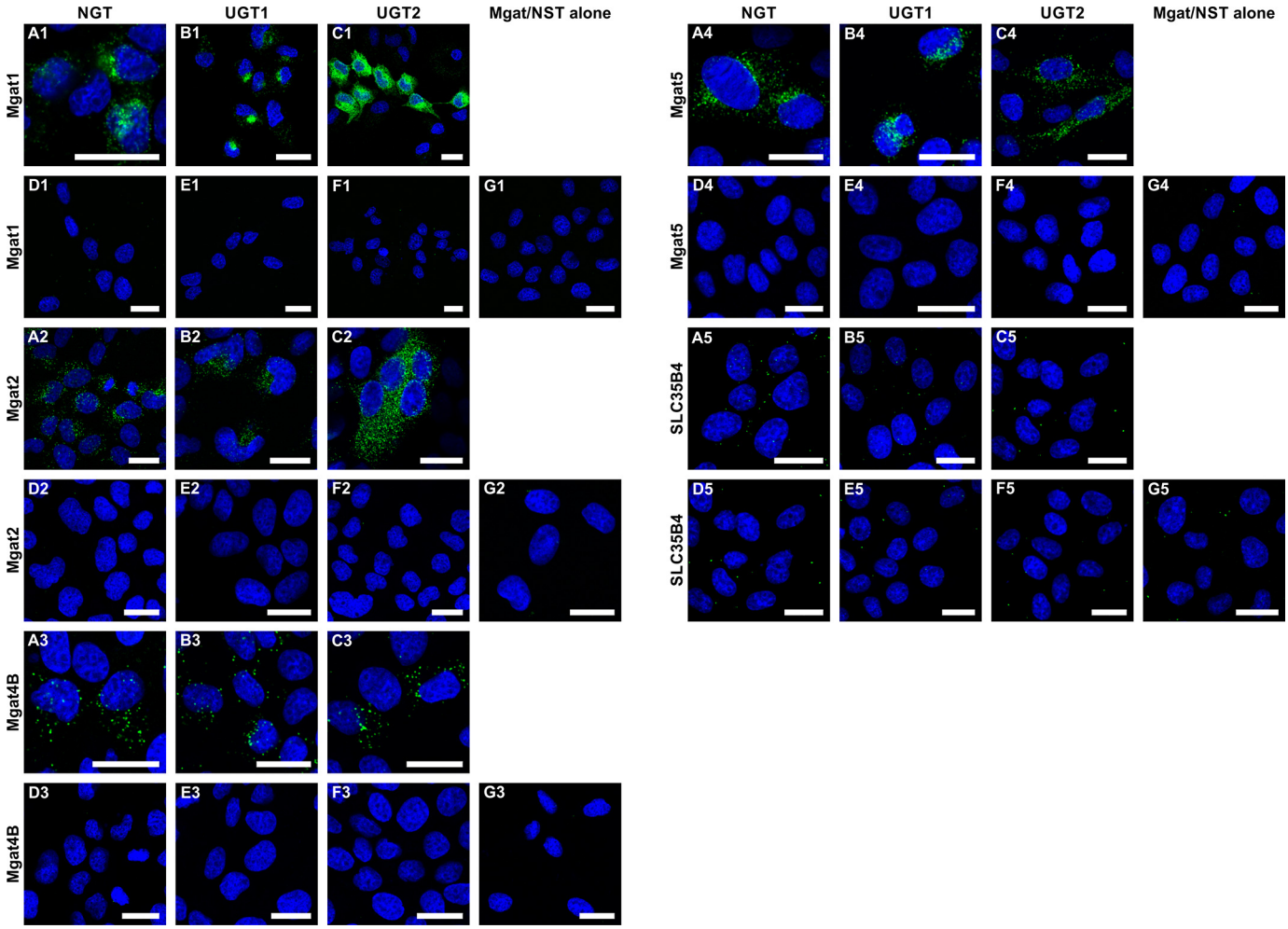

FIGURE 3. **Visualization of interactions between overexpressed Mgats and UDP-sugar transporters using *in situ* PLA.** *A–C*, PLA analysis of either Mgat1 (*panels 1*), Mgat2 (*panels 2*), Mgat4B (*panels 3*), Mgat5 (*panels 4*), or SLC35B4 (*panels 5*) putative interaction with NGT (*A*), UGT1 (*B*), and UGT2 (*C*). *D*, negative control for HA-NGT and FLAG-Mgats/SLC35B4 interaction analysis, where primary antibodies were not added during the PLA procedure. *E*, negative control for HA-UGT1 and FLAG-Mgats/SLC35B4 interaction analysis, where primary antibodies were not added during the PLA procedure. *F*, negative control for HA-UGT2 and FLAG-Mgats/SLC35B4 interaction analysis, where primary antibodies were not added during the PLA procedure. *G*, negative control for HA-tagged UDP-sugar transporters and FLAG-Mgats/SLC35B4 interaction analysis, where MDCK-RCA^r cells expressing only FLAG-Mgats/SLC35B4 were used, and anti-FLAG antibody was omitted during the PLA procedure. *Bars*, 20 μm.

positive PLA signal was observed as well, thus confirming close proximity of both termini of the UGT protein and, more importantly, reliability of the PLA approach (Fig. 1).

To examine the close proximity between endogenous Mgat1/Mgat2/Mgat4B/Mgat5 and endogenous UGT/NGT, respective antibodies listed in Table 2 were used. Simultaneously, we performed negative controls where either only one or no primary antibody was added (Fig. 2, *C* and *D*). We found that all analyzed Mgats are in the neighborhood of both UGT (Fig. 2*A*) and NGT (Fig. 2*B*). Importantly, this is the first report demonstrating interactions occurring between endogenous glycosyltransferases and NSTs. However, it should be noted that the above-described experiments do not distinguish between UGT splice variants (UGT1 and UGT2). Therefore, interactions occurring between UGT1 or UGT2 and Mgats could be detected using recombinantly expressed and tagged proteins only.

MDCK-RCA^r cells were stably transfected with plasmid encoding either Mgat1, Mgat2, Mgat4B, or Mgat5 in fusion with 3×FLAG epitope, and then clones were selected. In the next step, selected clones expressing FLAG-tagged Mgats were transiently transfected with plasmid encoding either NGT, UGT1, or UGT2 in fusion with HA peptide. Expression of UDP-sugar transporters was confirmed 24 h after transfection with immunofluorescence microscopy (data not shown). These cells were analyzed using PLA 48 h after transient transfection. We confirmed that all analyzed Mgats are in close proximity to NGT. Moreover, we found that they are in the neighborhood of both splice variants of UGT, UGT1, and UGT2 (Fig. 3, *A–C*).

A procedure similar to the one described above was employed to analyze putative proximity between SLC35B4 and NGT, UGT1, and UGT2. We considered the SLC35B4/UGT2 protein combination as a negative control because of the FLIM-negative results for this pair of proteins (15), whereas the SLC35B4/NGT combination was used as a negative control in the co-immunoprecipitation approach (13). Although SLC35B4 belongs to the group of proteins comprising nucleotide sugar transporters and is homologous to the transporters examined in this study (NGT, UGT1, and UGT2), PLA did not result in any positive signal in all three analyzed

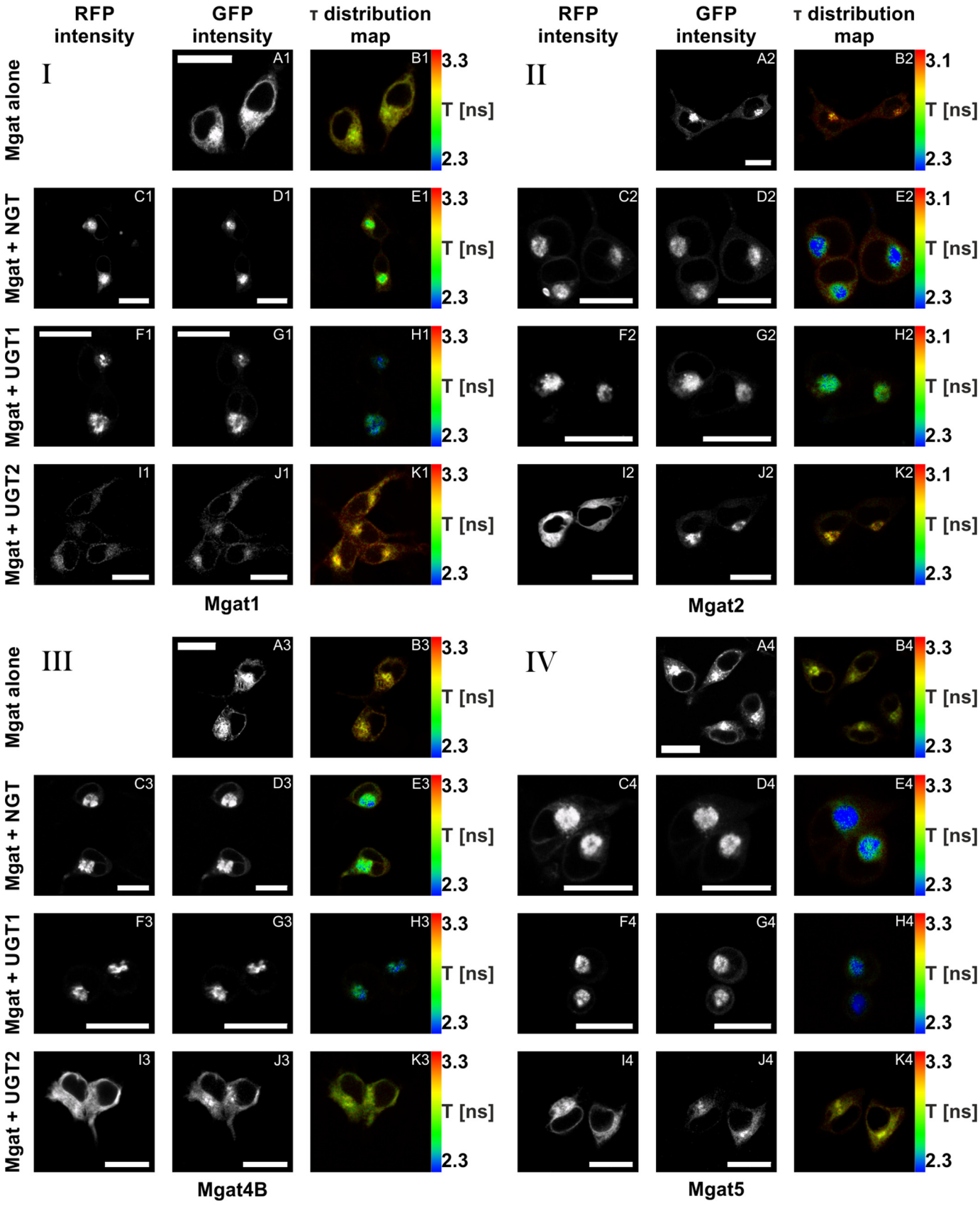
RFP intensity
GFP intensity
τ distribution map
I
II
III
IV
Mgat alone
Mgat + NGT
Mgat + UGT1
Mgat + UGT2
A1
B1
C1
D1
E1
F1
G1
H1
I1
J1
K1
A2
B2
C2
D2
E2
F2
G2
H2
I2
J2
K2
A3
B3
C3
D3
E3
F3
G3
H3
I3
J3
K3
A4
B4
C4
D4
E4
F4
G4
H4
I4
J4
K4
3.3
3.1
T [ns]
2.3
Mgat1
Mgat2
Mgat4B
Mgat5

NST combinations (Fig. 3, *panels A5–G5*), suggesting that the examined interactions between other proteins did not result from overexpression artifacts and that high degree of homology, as well as common subcellular localization of those multitransmembrane proteins, are not sufficient for their occurrence in close proximity.

To confirm the obtained results, technical negative controls were also employed. First, the negative control employed MDCK-RCA^r cells expressing both proteins but instead of HA- and FLAG-specific primary antibodies incubation with 10% (v/v) normal goat serum solution was applied. The rest of the protocol was not changed (Fig. 3, *D*, *E*, and *G*). The second negative control involved MDCK-RCA^r cells expressing 3×FLAG-Mgat only. During PLA with these cells anti-FLAG antibody was omitted (Fig. 1*B* and Fig. 3*G*). As an additional negative control, we considered cells that were not transfected with expression plasmids encoding UDP-sugar transporters because of limited efficiency of transient transfection and stained with the regular PLA protocol. These cells (Figs. 1*C* and 3, *A–C*), as well as the other negative controls examined, did not show any (or showed a significantly lower) signal.

FLIM-FRET Analysis Demonstrates Extensive Interactions between Mgats and UDP-Sugar Transporters—HEK293T cells were transiently transfected with plasmids enabling expression of eGFP-Mgats and mRFP-UDP-sugar transporters (Table 1). All analyzed eGFP-Mgats localized mainly to the Golgi apparatus. However, a significant pool could be assigned to the ER, obviously resulting from both the ongoing biosynthesis and Golgi to ER recycling of Mgat fusion proteins (Fig. 4, *A*, *D*, *G*, and *J*). When co-expressed with eGFP-Mgats, both mRFP-NGT and mRFP-UGT1 localized predominantly to the Golgi apparatus (Fig. 4, *C* and *F*), whereas mRFP-UGT2 localized mainly to the ER (Fig. 4*I*). Co-expression with mRFP-tagged NGT and UGT1 caused an indisputable increase in Golgi-localized eGFP-Mgat pools with concomitant diminution of the ER-derived signals (Fig. 4, *D* and *G*). Upon co-expression with mRFP-UGT2 all eGFP-Mgats could be readily detected within the ER (Fig. 4*J*), which was especially pronounced in the case of Mgat4B.

In the FLIM-FRET approach, a reduction in the fluorescence lifetime (τ) of the donor fluorophore in the presence of the acceptor fluorophore indicates interaction between analyzed fusion proteins (fluorescence lifetime of the donor fluorophore in the absence of the acceptor fluorophore is considered as a reference). Fig. 4 demonstrates mean lifetime of eGFP-tagged Mgat1 (Fig. 4*B1*), Mgat2 (Fig. 4*B2*), Mgat4B (Fig. 4*B3*), and Mgat5 (Fig. 4*B4*) in the absence of an acceptor fluorophore. Co-expression of eGFP-tagged Mgats both with mRFP-NGT and mRFP-UGT1 resulted in a statistically significant reduction of GFP fluorescence lifetime. Interestingly, co-expression with mRFP-UGT2 shortened the GFP fluorescence lifetime only in the case of eGFP-Mgat4B. The other eGFP-Mgats did not show any reduction of GFP lifetime upon mRFP-UGT2 co-expression (Fig. 4, *E*, *H*, and *K*). Fig. 5 shows mean fluorescence lifetime of either eGFP-Mgat1 (Fig. 5*A*), eGFP-Mgat2 (Fig. 5*B*), eGFP-Mgat4B (Fig. 5*C*), or eGFP-Mgat5 (Fig. 5*D*) upon mRFP-NGT, mRFP-UGT1, or mRFP-UGT2 co-expression.

In all FRET-positive Mgat-UDP-sugar transporter combinations, a bi-exponential model was employed to analyze the data. This model allows two lifetime components to be distinguished: a longer one assumed to be equal to the τ value of the control measurements and resulting from the presence of a noninteracting donor fraction and a shorter one that corresponds to the donor fraction interacting with the acceptor. The data obtained for control measurements as well as for noninteracting proteins were analyzed using mono-exponential model.

Interestingly, average GFP lifetime was always shorter for UGT1-Mgats than for NGT-Mgats co-expression, except for Mgat5 simultaneous expression with these proteins (Fig. 5, *A–D*). Nonetheless, fluorescence lifetime of the interacting donor fraction (τ_{short}) was always shorter for NGT-Mgats co-expression. The difference was observed because the fraction of UGT1 interacting with Mgats was significantly higher (~50% of the donor usually occurs in close proximity to the acceptor) than for NGT (from 18 up to 39% of the donor interacts with the acceptor) (Table 3). Three of twelve analyzed protein combinations did not result in a decrease in GFP fluorescence lifetime (eGFP-Mgat1/Mgat2/Mgat5 + mRFP-UGT2). These combinations could be therefore considered as negative controls, additionally confirming positive results obtained in this experiment.

Mean FRET Efficiency May Reflect Putative Distances between Analyzed Proteins—Mean FRET efficiency is a value calculated from the equation: $1 - (\tau_{short}/\tau_{long})$. This value corresponds to the distance between the donor and the acceptor. However, it is crucial to note that the calculated distance will refer to eGFP and mRFP rather than to investigated protein pairs. Moreover, because data on the NST structure is still missing, it is impossible to assign the exact position of the eGFP-tagged N-terminal cytosolic stretches in the context of the entire molecule. That is why we decided not to calculate the exact distance between Mgats and UDP-sugar transporters. Nonetheless, based on the significant differences in mean FRET efficiency between investigated protein combinations, we attempted to estimate which Mgats are closer and which are further from examined NSTs, assuming that the longer the distance between two interacting fluorophores, the lower the mean FRET efficiency value (Table 4 and Fig. 5*E*). We demonstrated that Mgat1 is in the close vicinity of both NGT and UGT1. The only Mgat that appears to directly interact with

FIGURE 4. ***In vivo* FLIM-FRET analysis of interactions between Mgats and UDP-sugar transporters.** *A–K*, confocal intensity-resolved (*A*, *C*, *D*, *F*, *G*, *I*, and *J*) and time-resolved (*B*, *E*, *H*, and *K*) imaging of eGFP-Mgat (*D*, *G*, and *J*) interaction with mRFP-UDP-sugar transporter (*C*, *F*, and *I*) in HEK293T cells in comparison with cells expressing eGFP-Mgat only (*A*). FLIM-FRET analysis of either Mgat1 (*panel I*), Mgat2 (*panel II*), Mgat4B (*panel III*), or Mgat5 (*panel IV*) putative interactions with NGT (*C–E*), UGT1 (*F–H*), and UGT2 (*I–K*). GFP fluorescence lifetime (τ) was shortened by simultaneous overexpression of eGFP-Mgats with both mRFP-NGT and mRFP-UGT1, strongly suggesting an interaction between these proteins. In the case of mRFP-UGT2, the same phenomenon was demonstrated only upon eGFP-Mgat4B co-expression. Co-expression of mRFP-UGT2 with eGFP-Mgat1, Mgat2, and Mgat5 did not influence GFP fluorescence lifetime. The *red* to *blue* color shift reflects shortening of the fluorescence lifetime. The *rainbow scale bars* placed next to time-resolved images (*B*, *E*, *H*, and *K*) represent fluorescence lifetime range between either 2.3 (*blue*) and 3.3 ns (*red*; Mgat1, Mgat4B, or Mgat5) or 2.3 (*blue*) and 3.1 ns (*red*; Mgat2). *Bars*, 20 μm. τ, fluorescence lifetime.

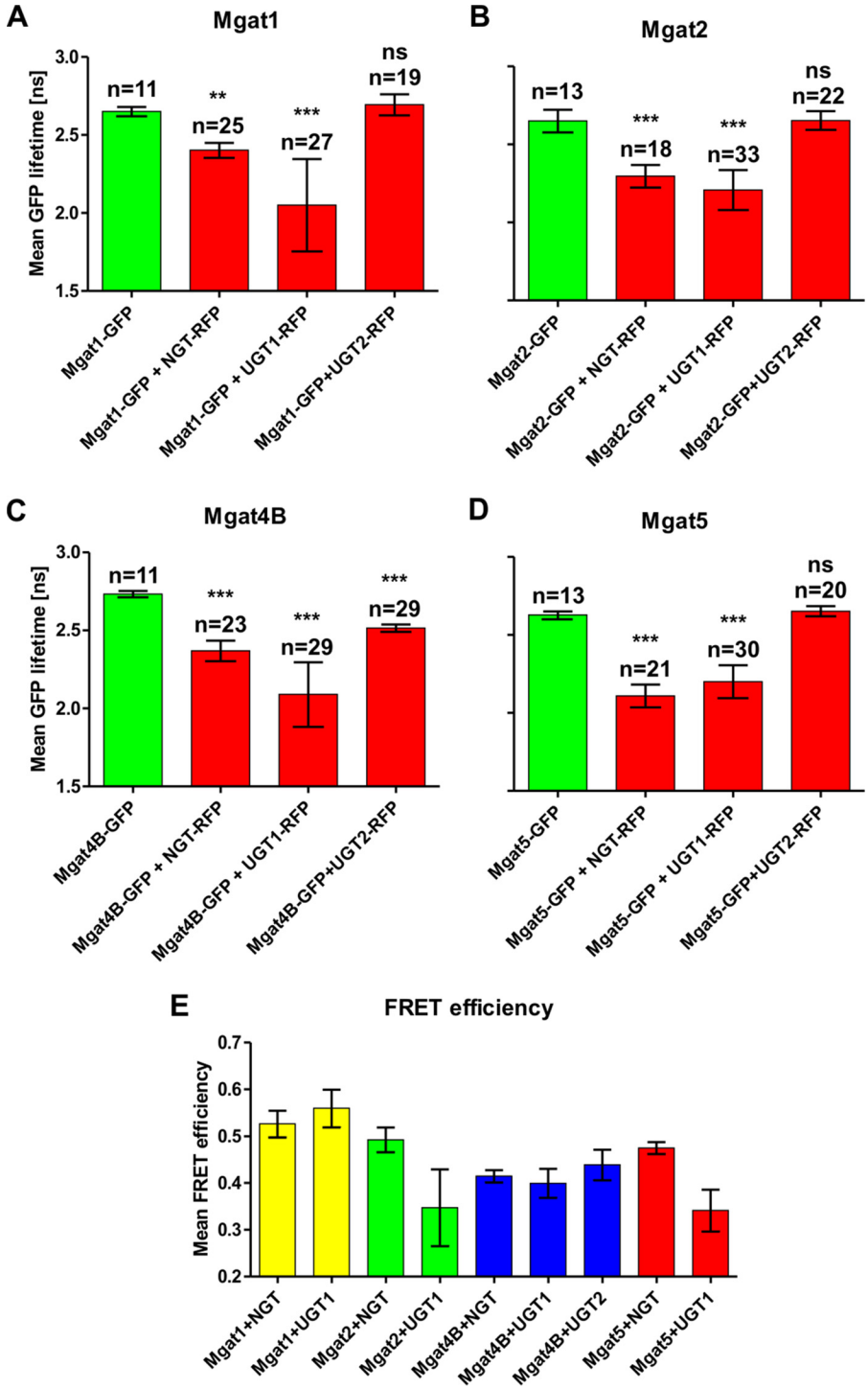

FIGURE 5. ***In vivo* FLIM-FRET analysis of interactions between Mgats and UDP-sugar transporters.** *A–D*, mean GFP lifetime values in the absence and in the presence of acceptor are shown. The data are shown as means ± S.D. from several measurements of the indicated cell number (*n*). Statistically significant (one-way analysis of variance test, $p < 0.001$) reduction of GFP lifetime upon co-expression of fluorophore-tagged Mgats and NGT, as well as UGT1, was demonstrated by comparing with eGFP-Mgats alone. No difference in GFP lifetime was observed when mRFP-UGT2 and eGFP-Mgat1, eGFP-Mgat2, and eGFP-Mgat5 were co-expressed. Only upon simultaneous expression of mRFP-UGT2 and eGFP-Mgat4B was a statistically significant decrease in GFP lifetime observed. *E*, mean FRET efficiency calculated for the FRET-positive Mgat-UDP-sugar transporter combinations. The data are shown as means ± S.D. from several measurements of the indicated (*A–D*) cell number (*n*). Mean FRET efficiency was calculated to estimate relative distances between interacting proteins (the higher the mean FRET efficiency, the shorter the distance between two proteins).

UGT2, namely Mgat4B, is at the same time the most distant from NGT. On the other hand, Mgat1 and Mgat4B are more proximally located toward UGT1 than Mgat2 and Mgat5. Interestingly, the distance between Mgats and UGT1 appears to be more variable compared with NGT. This may arise from a difference in the length of cytosolically exposed N-terminal stretches between these NSTs. The significantly longer N-terminal stretch of UGT1 (36 amino acids) most likely results in

TABLE 3
In vivo **FLIM-FRET analysis of interactions between UDP-sugar transporters and Mgats**

FRET combinations	*n*	$\tau_{average}$	τ_{short}	f_{short}	τ_{long}	χ^2
		ns	*ns*		*ns*	
eGFP-Mgat1 alone	11	2.65 ± 0.03		0.0	2.65 ± 0.03	0.99 ± 0.05
eGFP-Mgat1 + mRFP-NGT	25	2.40 ± 0.05	1.26 ± 0.10	0.18 ± 0.04	2.65	1.00 ± 0.05
eGFP-Mgat1 + mRFP-UGT1	27	2.05 ± 0.30	1.29 ± 0.22	0.44 ± 0.20	2.65	1.04 ± 0.06
eGFP-Mgat1 + mRFP-UGT2	19	2.69 ± 0.07		0.0	2.69 ± 0.07	1.03 ± 0.03
eGFP-Mgat2 alone	13	2.65 ± 0.07		0.0	2.65 ± 0.07	1.00 ± 0.02
eGFP-Mgat2 + mRFP-NGT	18	2.30 ± 0.07	1.34 ± 0.07	0.27 ± 0.05	2.65	1.04 ± 0.06
eGFP-Mgat2 + mRFP-UGT1	33	2.21 ± 0.13	1.65 ± 0.27	0.51 ± 0.25	2.65	1.02 ± 0.07
eGFP-Mgat2 + mRFP-UGT2	22	2.65 ± 0.06		0.0	2.65 ± 0.06	1.05 ± 0.05
eGFP-Mgat4B alone	11	2.73 ± 0.02		0.0	2.73 ± 0.02	1.02 ± 0.07
eGFP-Mgat4B + mRFP-NGT	23	2.37 ± 0.07	1.58 ± 0.06	0.31 ± 0.05	2.73	0.97 ± 0.05
eGFP-Mgat4B + mRFP-UGT1	29	2.09 ± 0.20	1.64 ± 0.11	0.58 ± 0.14	2.73	1.02 ± 0.07
eGFP-Mgat4B + mRFP-UGT2	29	2.52 ± 0.02	1.53 ± 0.12	0.18 ± 0.03	2.73	1.01 ± 0.06
eGFP-Mgat5 alone	13	2.63 ± 0.02		0.0	2.63 ± 0.02	1.04 ± 0.01
eGFP-Mgat5 + mRFP-NGT	21	2.11 ± 0.07	1.38 ± 0.04	0.39 ± 0.07	2.63	1.00 ± 0.06
eGFP-Mgat5 + mRFP-UGT1	30	2.20 ± 0.10	1.75 ± 0.22	0.52 ± 0.20	2.63	1.03 ± 0.07
eGFP-Mgat5 + mRFP-UGT2	20	2.65 ± 0.03		0.0	2.65 ± 0.03	1.04 ± 0.06

TABLE 4
Mean FRET efficiencies calculated for pairs of Mgats and UDP-sugar transporters interacting on FLIM-FRET

FRET combinations	Mean FRET efficiency
eGFP-Mgat1 + mRFP-NGT	0.524 ± 0.039
eGFP-Mgat1 + mRFP-UGT1	0.521 ± 0.082
eGFP-Mgat2 + mRFP-NGT	0.492 ± 0.026
eGFP-Mgat2 + mRFP-UGT1	0.376 ± 0.102
eGFP-Mgat4B + mRFP-NGT	0.423 ± 0.021
eGFP-Mgat4B + mRFP-UGT1	0.402 ± 0.042
eGFP-Mgat4B + mRFP-UGT2	0.441 ± 0.043
eGFP-Mgat5 + mRFP-NGT	0.478 ± 0.014
eGFP-Mgat5 + mRFP-UGT1	0.333 ± 0.080

greater motility of the attached fluorophore compared with NGT (6 amino acids).

Mannoside Acetylglucosaminyltransferases and Nucleotide Sugar Transporters Form Heterooligomeric Complexes—According to the values corresponding to interacting fractions (f_{short}), Mgat1, Mgat2 and Mgat4B form approximately twice as many complexes with UGT1 as with NGT (Table 3). It therefore appears that UGT1 associates with Mgats even to a greater extent than NGT. We can also observe a gradual increase of the NGT-interacting fraction from Mgat1 to Mgat5. The same is true for UGT1, except Mgat5, for which a slight decrease in the UGT1-interacting fraction occurs. This may mean that Mgat1 and Mgat2 are able to interact with a wider range of proteins than Mgat4B and Mgat5. Interestingly, co-expression of respective Mgats with NGT or UGT1 appears to increase Golgi-localized Mgat pools. Overall FLIM-FRET results strongly suggest that Golgi localization of enzymes acting late in the *N*-glycan branching pathway is more dependent on the association with NSTs compared with the early acting ones. This phenomenon could additionally account for the reduced *N*-glycan branching upon NGT knockdown (15), because the expression of endogenous Mgats has been shown to decrease from Mgat1 to Mgat5 (41). Therefore, one may assume that NGT deficiency would affect Golgi localization of Mgat4B and Mgat5 to a greater extent than of Mgat1 and Mgat2, possibly having more interacting partners able to retain them in the Golgi apparatus upon reduced NGT availability. Moreover, it is highly probable that NGT knockdown disrupts NGT/UGT complexes, resulting in a decrease of Golgi-localized UGT fraction, which could also contribute to mislocalization of Mgat4B and Mgat5. This would strongly suggest that the ability of UDP-sugar transporters to interact with Mgats plays an important role in regulation of the *N*-glycan branching pathway. PLA demonstrated that Mgat2/UGT2, Mgat4B/UGT2, and Mgat5/UGT2 complexes are found exclusively in the ER of UGT-deficient MDCK-RCA^r cells (Fig. 3, *panels C2–C4*). Interestingly, according to FLIM-FRET results, Mgat1, Mgat2, and Mgat5 do not interact with UGT2 directly. We therefore assume that this phenomenon is mediated by an as yet unidentified endogenous protein. The most probable candidate is NGT, which interacts with all analyzed Mgats, and this interaction is detected both at the endogenous protein level and upon overexpression. Moreover, NGT undergoes similar UGT2-dependent relocation (Ref. 13 and our unpublished data). Somewhat different behavior is displayed by Mgat1, because a significant pool of Mgat1/UGT2 complexes is detected in the Golgi apparatus (Fig. 3*C1*). It has been reported that Mgat1 is involved in maintenance of proper Golgi structure and morphology (42), which might possibly explain partial Golgi retention of Mgat1/UGT2 complexes. Interestingly, co-expression of Mgat4B with UGT1 and NGT in UGT-deficient MDCK-RCA^r cells appears to relocate these Golgi-resident NSTs to the ER (Fig. 3*A*, *panels 3–5*). This phenomenon might be mediated by a di-lysine motif occurring at the C terminus of the Mgat4B amino acid sequence (KKAD), which may act as an ER retrieval signal. According to FLIM-FRET results obtained using the HEK293T cell line, an interaction between Mgat4B and UGT1, as well as NGT occurs mainly in the Golgi apparatus (Fig. 4, *panels E3* and *H3*). Therefore, it appears that Mgat4B *per se* is retrieved to the ER and may require co-expression of all examined NSTs (NGT, UGT1, and UGT2) to achieve Golgi localization. Mgat4B is the only Mgat that appears to directly interact with UGT2 (Figs. 4 and 5), and mean FRET efficiency values suggest that this interaction is even closer than that with UGT1. Interestingly, this is the most NGT-distant Mgat (Fig. 5*E*), which may in part explain inhibition of *N*-glycan branching caused by NGT knockdown (15). We assume that in NGT-deficient cells endogenous Mgat4B preferentially interacts with UGT2, which enhances the intrinsic tendency of the former to be retrieved to the ER unlike other Mgats, which are retained in the Golgi apparatus because of a more favorable association with UGT1. Because complexes formed by all examined NSTs with Mgat4B appear less abundant compared with other Mgats (Fig. 3, *panels A3*, *B3*, and *C3*),

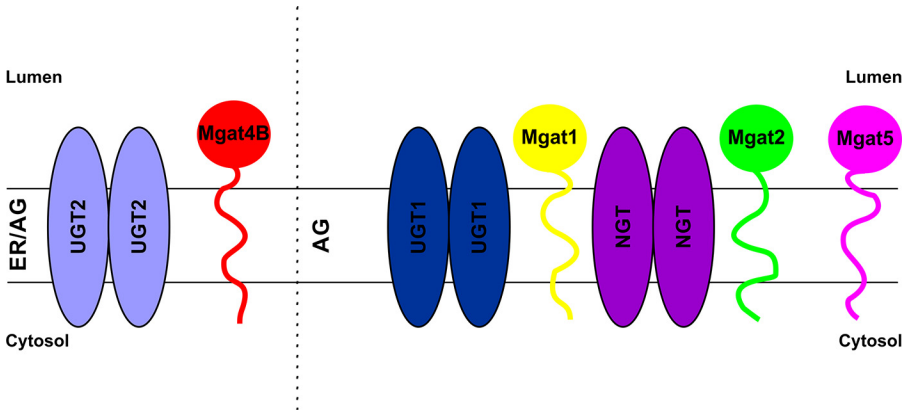

FIGURE 6. **Schematic representation of complex formation between UDP-sugar transporters and Mgats.** We hypothesize that in the ER UDP-sugar transporters recruit glycosyltransferase homodimers of one type at a time and accompany them on their way to the target Golgi compartment, where subsequent association of incoming NSTs brings distinct glycosyltransferase homodimers together, thus enabling a rearrangement that results in glycosyltransferase heterooligomerization. *ER*, endoplasmic reticulum; *AG*, Golgi apparatus.

it is highly probable that ER relocation of this enzyme would result in a significant reduction of *N*-glycan branching. Therefore, our findings may reveal a completely novel mechanism involved in the control of this physiologically relevant pathway.

Interestingly, a positive signal in *in situ* PLA experiments was also clearly visible for three FLIM-FRET-negative combinations (UGT2 + Mgat1, Mgat2, or Mgat5). Because the FLIM-FRET approach detects interactions between proteins that are separated by a distance no longer than 10 nm, whereas PLA technique demonstrates protein interactions occurring up to 40 nm, it is possible to obtain positive results using PLA for FRET-negative combinations. This strongly suggests that the distances between UGT2 and Mgat1, Mgat2, and Mgat5 are in the range of 10–40 nm. Therefore, combination of these two techniques is suitable to distinguish between proteins present in the same complex but not necessarily occurring next to each other.

Close proximity between UDP-*N*-acetylglucosamine-specific enzymes and UGT is surprising, because galactosyltransferase I appears to be absent from detergent-insoluble Mgat1-containing complexes (43, 44). Physical separation of galactosyltransferase I from Mgats is proposed to additionally support *N*-glycan branching, because Mgat4 and Mgat5 are unable to modify galactosylated acceptors (45, 46). Therefore, possible involvement in galactosylation barely explains UGT association with Mgats. We hypothesize that UGT and NGT act as multitransmembrane tethers linking Mgats involved in consecutive glycosylation reactions, thus enabling lateral extension of such putative Golgi-located complexes. UGT and NGT have been reported to form homooligomers (12, 13). Moreover, NGT has been shown to interact with UGT1 and UGT2, and both UGT splice variants associate as well (13). On the other hand, homooligomerization was reported for Mgat1 and Mgat2 (35), as well as Mgat5 (47). Mgat1 interactions with α1,3–1,6 mannosidase II (48) and Mgat2 (49) have also been demonstrated. Although direct evidence for the co-existence of all these proteins within one complex is currently missing, their remarkable homo- and heterooligomerization capacity encouraged us to propose that Golgi membranes contain large multiprotein complexes composed of multiple distinct NSTs, glycosyltransferases, and other glycosylation-related proteins (Fig. 6). Because of presence of such complexes, *N*-glycan branching could be performed in a highly coordinated fashion, because glycosylated acceptors might be effectively and precisely channeled from one enzyme to another. Based on this idea, we predict that the nascent oligosaccharide structure would be dictated by the qualitative and quantitative composition of such multiprotein complexes.

It has been reported that *medial* Golgi glycosyltransferases exist within high molecular mass complexes (43). These structures appear to exceed 1 MDa, but their exact molecular masses and composition have not been determined. Among proteins forming these extensive complexes, Mgat1 and Mgat2 have been identified. Slusarewicz *et al.* (44) isolated matrix linking adjacent cisternae of the medial Golgi compartment, which tightly binds Mgat1 and α1,3–1,6 mannosidase II. Interestingly, solubilization of these structures required high ionic strength (43, 44). In this study we demonstrated that NGT, UGT1, and UGT2 might form these complexes as well. Importantly, we were able to co-immunoprecipitate NGT, UGT1, and UGT2 using a salt-free buffer only (13). Buffers containing 150 mM NaCl reduced co-purification efficiency, whereas buffers containing 500 mM NaCl completely precluded co-immunoprecipitation (our unpublished data). This supports the idea that NGT and UGT are also constituents of high molecular mass complexes described by others (43, 44).

Conclusions—In this study we identified 11 previously unrecognized heterooligomeric complexes formed between NSTs and glycosyltransferases, and we proved that they occur at the endogenous protein level as well. We demonstrated that UDP-sugar transporters are able to interact with four distinct Mgats. Interestingly, these enzymes associate not only with functionally related NGT, but also with UGT, which is believed to be involved in the subsequent stage of glycosylation. We propose that NGT, UGT, and Mgats form large complexes in the Golgi membrane that could significantly facilitate biosynthesis of complex *N*-glycans. Although confirmation of this hypothesis requires further investigation, the discovery of the remarkable ability of NSTs to interact with each other and with distinct

glycosyltransferases may be a breakthrough in our understanding of glycosylation processes and their regulation. Moreover, because subcellular localization of Mgats appears to largely depend on close proximity to NSTs, these multitransmembrane proteins might be the key players in glycosylation of macromolecules.

References

1. Hadley, B., Maggioni, A., Ashikov, A., Day, C. J., Haselhorst, T., and Tiralongo, J. (2014) Structure and function of nucleotide sugar transporters: current progress. *Comput. Struct. Biotechnol. J.* **10,** 23–32
2. Coates, S. W., Gurney, T., Jr., Sommers, L. W., Yeh, M., and Hirschberg, C. B. (1980) Subcellular localization of sugar nucleotide synthetases. *J. Biol. Chem.* **255,** 9225–9229
3. Münster, A. K., Eckhardt, M., Potvin, B., Mühlenhoff, M., Stanley, P., and Gerardy-Schahn, R. (1998) Mammalian cytidine 5′-monophosphate *N*-acetylneuraminic acid synthetase: a nuclear protein with evolutionarily conserved structural motifs. *Proc. Natl. Acad. Sci. U.S.A.* **95,** 9140–9145
4. Gerardy-Schahn, R., Oelmann, S., and Bakker, H. (2001) Nucleotide sugar transporters: Biological and functional aspects. *Biochimie* **83,** 775–782
5. Caffaro, C. E., and Hirschberg, C. B. (2006) Nucleotide sugar transporters of the Golgi apparatus: from basic science to diseases. *Acc. Chem. Res.* **39,** 805–812
6. Capasso, J. M., and Hirschberg, C. B. (1984) Mechanism of glycosylation and sulfation in the Golgi apparatus: evidence for nucleotide sugar/nucleoside monophosphate and nucleotide sulfate/nucleoside monophosphate antiports in the Golgi apparatus membrane. *Proc. Natl. Acad. Sci. U.S.A.* **81,** 7051–7055
7. Eckhardt, M., Gotza, B., and Gerardy-Schahn, R. (1999) Membrane topology of the mammalian CMP-sialic acid transporter. *J. Biol. Chem.* **274,** 8779–8787
8. Abe, M., Hashimoto, H., and Yoda, K. (1999) Molecular characterization of Vig4/Vrg4 GDP-mannose transporter of the yeast *Saccharomyces cerevisiae*. *FEBS Lett.* **458,** 309–312
9. Puglielli, L., and Hirschberg, C. B. (1999) Reconstitution, identification and purification of the rat liver Golgi membrane GDP-fucose transporter. *J. Biol. Chem.* **274,** 35596–35600
10. Puglielli, L., Mandon, E. C., Rancour, D. M., Menon, A. K., and Hirschberg, C. B. (1999) Identification and purification of the rat liver Golgi membrane UDP-*N*-acetylgalactosamine transporter. *J. Biol. Chem.* **274,** 4474–4479
11. Hong, K., Ma, D., Beverley, S. M., and Turco, S. J. (2000) The *Leishmania* GDP-mannose transporter is an autonomous, multispecific, hexameric complex of LPG2 subunits. *Biochemistry* **39,** 2013–2022
12. Olczak, M., and Guillen, E. (2006) Characterization of a mutation and an alternative splicing of UDP-galactose transporter in MDCK-RCA^r cell line. *Biochim Biophys Acta* **1763,** 82–92
13. Maszczak-Seneczko, D., Sosicka, P., Majkowski, M., Olczak, T., and Olczak, M. (2012) UDP-*N*-acetylglucosamine transporter and UDP-galactose transporter form heterologous complexes in the Golgi membrane. *FEBS Lett.* **586,** 4082–4087
14. Sprong, H., Degroote, S., Nilsson, T., Kawakita, M., Ishida, N., van der Sluijs, P., and van Meer, G. (2003) Association of the Golgi UDP-galactose transporter with UDP-galactose:ceramide galactosyltransferase allows UDP-galactose import in the endoplasmic reticulum. *Mol. Biol. Cell* **14,** 3482–3493
15. Maszczak-Seneczko, D., Sosicka, P., Olczak, T., Jakimowicz, P., Majkowski, M., and Olczak, M., (2013) UDP-*N*-acetylglucosamine transporter (SLC35A3) regulates biosynthesis of highly branched *N*-glycans and keratan sulfate. *J. Biol. Chem.* **288,** 21850–21860
16. Miura, N., Ishida, N., Hoshino, M., Yamauchi, M., Hara, T., Ayusawa, D., and Kawakita, M. (1996) Human UDP-galactose translocator: molecular cloning of a complementary DNA that complements the genetic defect of a mutant cell line deficient in UDP-galactose translocator. *J. Biochem.* **120,** 236–241
17. Ishida, N., Miura, N., Yoshioka, S., and Kawakita, M. (1996) Molecular cloning and characterization of a novel isoform of the human UDP-galactose transporter, and of related complementary DNAs belonging to the nucleotide-sugar transporter gene family. *J Biochem.* **120,** 1074–1078
18. Oelmann, S., Stanley, P., and Gerardy-Schahn, R. (2001) Point mutations identified in Lec8 Chinese hamster ovary glycosylation mutants that inactivate both the UDP-galactose and CMP-sialic acid transporters. *J. Biol. Chem.* **276,** 26291–26300
19. Maszczak-Seneczko, D., Olczak, T., Wunderlich, L., and Olczak, M. (2011) Comparative analysis of involvement of UGT1 and UGT2 splice variants of UDP-galactose transporter in glycosylation of macromolecules in MDCK and CHO cell lines. *Glycoconj. J.* **28,** 481–492
20. Brändli, A. W., Hansson, G. C., Rodriguez-Boulan, E., and Simons K (1988) A polarized epithelial cell mutant deficient in translocation of UDP-galactose into the Golgi complex. *J. Biol. Chem.* **263,** 16283–16290
21. Stanley, P. (1983) Lectin-resistant CHO cells: selection of new mutant phenotypes. *Somatic Cell Genet.* **9,** 593–608
22. Hara, T., Endo, T., Furukawa, K., Kawakita, M., and Kobata, A. (1989) Elucidation of the phenotypic change on the surface of Had-1 cell, a mutant cell line of mouse FM3A carcinoma cells selected by resistance to Newcastle disease virus infection. *J. Biochem.* **106,** 236–247
23. Yoshioka, S., Sun-Wada, G. H., Ishida, N., and Kawakita, M. (1997) Expression of the human UDP-galactose transporter in the Golgi membranes of murine Had-1 cells that lack the endogenous transporter. *J. Biochem.* **122,** 691–695
24. Maszczak-Seneczko, D., Olczak, T., and Olczak, M. (2011) Subcellular localization of UDP-GlcNAc, UDP-Gal and SLC35B4 transporters. *Acta Biochim. Pol.* **58,** 413–419
25. Maszczak-Seneczko, D., Olczak, T., Jakimowicz, P., and Olczak, M. (2011) Overexpression of UDP-Glc*N*Ac transporter partially corrects galactosylation defect caused by UDP-Gal transporter mutation. *FEBS Lett.* **585,** 3090–3094
26. Olczak, M., Maszczak-Seneczko, D., Sosicka, P., Jakimowicz, P., and Olczak, T. (2013) UDP-Gal/UDP-GlcNAc chimeric transporter complements mutation defect in mammalian cells deficient in UDP-Gal transporter. *Biochem. Biophys. Res. Commun.* **434,** 473–478
27. Sosicka, P., Jakimowicz, P., Olczak, T., and Olczak, M. (2014) Short N-terminal region of UDP-galactose transporter (SLC35A2) is crucial for galactosylation of *N*-glycans. *Biochem. Biophys. Res. Commun.* **454,** 486–492
28. van den Eijnden, D., and Joziasse, D. H. (1993) Enzymes associated with glycosylation. *Curr. Opin. Struct. Biol.* **3,** 711–721
29. Schachter, H. (1994) Molecular cloning of glycosyltransferase genes. In *Molecular Glycobiology* (Fukuda, M., and Hindsgaul, O., eds) pp. 88–162, Oxford University Press, Oxford
30. Field, M. C., and Wainwright, L. J. (1995) Molecular cloning of eukaryotic glycoprotein and glycolipid glycosyltransferases: a survey. *Glycobiology* **5,** 463–472
31. Rabouille, C., Hui, N., Hunte, F., Kieckbusch, R., Berger, E. G., Warren, G., and Nilsson, T. (1995) Mapping the distribution of Golgi enzymes involved in the construction of complex oligosaccharides. *J. Cell Sci.* **108,** 1617–1627
32. Lau, K. S., and Dennis, J. W. (2008) *N*-Glycans in cancer progression. *Glycobiology* **18,** 750–760
33. Spessott, W., Crespo, P. M., Daniotti, J. L., and Maccioni, H. J. (2012) Glycosyltransferase complexes improve glycolipid synthesis. *FEBS Lett.* **586,** 2346–2350
34. Ferrari, M. L., Gomez, G. A., and Maccioni, H. J. (2012) Spatial organization and stoichiometry of N-terminal domain-mediated glycosyltransferase complexes in Golgi membranes determined by FRET microscopy. *Neurochem. Res.* **37,** 1325–1334
35. Hassinen, A., Rivinoja, A., Kauppila, A., and Kellokumpu, S. (2010) Golgi *N*-glycosyltransferases form both homo- and heterodimeric enzyme complexes in live cells. *J. Biol. Chem.* **285,** 17771–17777
36. Oikawa, A., Lund, C. H., Sakuragi, Y., and Scheller, H. V. (2013) Golgi-localized enzyme complexes for plant cell wall biosynthesis. *Trends Plant Sci.* **18,** 49–58
37. Schoberer, J., Liebminger, E., Botchway, S. W., Strasser, R., and Hawes, C. (2013) Time-resolved fluorescence imaging reveals differential interactions of *N*-glycan processing enzymes across the Golgi stack in planta. *Plant Physiol.* **161,** 1737–1754
38. Gao, X.-D., and Dean, N. (2000) Distinct protein domains of the yeast

Golgi GDP-mannose transporter mediate oligomer assembly and export from the endoplasmic reticulum. *J. Biol. Chem.* **275,** 17718–17727
39. Oguri, S., Yoshida, A., Minowa, M. T., and Takeuchi, M. (2006) Kinetic properties and substrate specificities of two recombinant human *N*-acetylglucosaminyltransferase-IV isozymes. *Glycoconj. J.* **23,** 473–480
40. Takamatsu, S., Antonopoulos, A., Ohtsubo, K., Ditto, D., Chiba, Y., Le, D. T., Morris, H. R., Haslam, S. M., Dell, A., Marth, J. D., and Taniguchi, N. (2010) Physiological and glycomic characterization of *N*-acetylglucosaminyltransferase-IVa and -IVb double deficient mice. *Glycobiology* **20,** 485–497
41. Lau, K. S., Partridge, E. A., Grigorian, A., Silvescu, C. I., Reinhold, V. N., Demetriou, M., and Dennis, J. W. (2007) Complex *N*-glycan number and degree of branching cooperate to regulate cell proliferation and differentiation. *Cell* **129,** 123–134
42. Nilsson, T., Rabouille, C., Hui, N., Watson, R., and Warren, G. (1996) The role of the membrane-spanning domain and stalk region of *N*-acetylglucosaminyltransferase I in retention, kin recognition and structural maintenance of the Golgi apparatus in HeLa cells. *J. Cell Sci.* **109,** 1975–1989
43. Opat, A. S., Houghton, F., and Gleeson, P. A. (2000) Medial Golgi but not late Golgi glycosyltransferases exist as high molecular weight complexes: role of luminal domain in complex formation and localization. *J. Biol. Chem.* **275,** 11836–11845
44. Slusarewicz, P., Nilsson, T., Hui, N., Watson, R., and Warren, G. (1994) Isolation of a matrix that binds medial Golgi enzymes. *J. Cell Biol.* **124,** 405–413
45. Cummings, R. D., Trowbridge, I. S., and Kornfeld, S. (1982) A mouse lymphoma cell line resistant to the leukoagglutinating lectin from *Phaseolus vulgaris* is deficient in UDP-Glc*N*Ac: α-D-mannoside β1,6 *N*-acetylglucosaminyltransferase. *J. Biol. Chem.* **257,** 13421–13427
46. Oguri, S., Minowa, M. T., Ihara, Y., Taniguchi, N., Ikenaga, H., and Takeuchi, M. (1997) Purification and characterization of UDP-*N*-acetylglucosamine: α1,3-D-mannoside β1,4-*N*-acetylglucosaminyltransferase (*N*-acetylglucosaminyltransferase-IV) from bovine small intestine. *J. Biol. Chem.* **272,** 22721–22727
47. Sasai, K., Ikeda, Y., Tsuda, T., Ihara, H., Korekane, H., Shiota, K., and Taniguchi, N. (2001) The critical role of the stem region as a functional domain responsible for the oligomerization and Golgi localization of *N*-acetylglucosaminyltransferase V: the involvement of a domain homophilic interaction. *J. Biol. Chem.* **276,** 759–765
48. Nilsson, T., Hoe, M. H., Slusarewicz, P., Rabouille, C., Watson, R., Hunte, F., Watzele, G., Berger, E. G., and Warren, G. (1994) Kin recognition between *medial* Golgi enzymes in HeLa cells. *EMBO J.* **13,** 562–574
49. Hassinen, A., Pujol, F. M., Kokkonen, N., Pieters, C., Kihlström, M., Korhonen, K., and Kellokumpu, S. (2011) Functional organization of Golgi *N*- and *O*-glycosylation pathways involves pH-dependent complex formation that is impaired in cancer cells. *J. Biol. Chem.* **286,** 38329–38340